ISSN: 2584-0495 Vol. 3, Issue 4, pp. 1621-1626

International Journal of Microsystems and IoT

ISSN: (Online) Journal homepage: https://www.ijmit.org

Machine-learning driven analysis of an Aluminum-based Plasmonic sensor in the Near-infrared region

R. Runthala, J. Jain, S. Shukla, and P. Arora

Cite as: Runthala, R., Jain, J., Shukla, S., & P. Arora, P. (2025). Machine-learning driven analysis of an Aluminum-based Plasmonic sensor in the Near-infrared region. International Journal of Microsystems and IoT, 3(4), 1621–1626. https://doi.org/10.5281/zenodo.18146753

Published online: 15 April 2025

https://doi.org/10.5281/zenodo.18146753

International Journal of Microsystems and IoT
Vol.3, Issue 4, pp.1621-1626; DOI: https://doi.org/10.5281/zenodo.18146753

Machine-learning driven analysis of an Aluminium-based Plasmonic sensor in the Near-infrared region

R. Runthala[1], J. Jain[1], S. Shukla[2], and P. Arora[1]

[1]Department of Electrical and Electronics Engineering, Birla Institute of Technology and Science, Pilani, Rajasthan, India.
[2] School of Computer Science, UPES Bidholi Campus, Dehradun, India

ABSTRACT
We present a multilayer SPR-based sensor capable of detecting analyte-induced changes in refractive index. The design incorporates an Aluminum-based prism with calcium fluoride, Silicon as the dielectric layer, and Fluorinated Graphene as the biorecognition element. The sensor is analyzed across the near-infrared region using the transfer matrix method, evaluating key parameters such as sensitivity (°/RIU) and figure of merit (1/RIU). Various machine learning regression models are applied to the curated dataset, compared using R^2 scores, and feature importance is investigated to provide new design insights. Testing on unseen inputs demonstrates that ML-based approaches can efficiently optimize sensor performance compared to conventional analytical methods.

KEYWORDS
Aluminium, plasmonic, machine learning, sensors, XgBoost, Random Forest, ANN

1. INTRODUCTION

Bio-sensing for real-world applications became feasible and convenient after the proliferation of label-free detection techniques [1]. In this view, nano-scale plasmonic detection has gained momentum for its accuracy and high sensing capabilities. Surface Plasmon Resonance (SPR) can be achieved through various methodologies, such as guided mode resonance [2], nano-structure arrangement [3], or prism metal interface, etc. Gold (Au), Silver (Ag), and Aluminium (Al) are the plasmonic metals used to satisfy the attenuated total internal reflection phenomenon to achieve such resonance at the metal-dielectric interface [2]. While utilizing these methodologies, a step-wise optimization of each of the intermediate geometrical parameters is required. Thus, the numerical analysis is done using simulation methods like Finite Difference Time Domain (FDTD) [4], Finite Element Analysis (FEM) [5] for the precise modeling of the electromagnetic interactions at the interface. These methods also consider the heterogeneity of the intermediate layers along with the complex boundary conditions, which becomes a very computationally intensive procedure. Given the wide range of operating wavelengths to work with these methods, there is always a chance of missing out on some combinations that might end up resulting in higher optical performance. Alternatively, if the physics behind the device is fixed, we can implement machine learning (ML)-based techniques to predict the patterns faster and more efficiently.

In other words, compiling a comprehensive database that systematically covers an entire range of input features, namely all possible combinations of the geometrical parameters involved, then applying ML to predict the performance parameters, appears to be a more efficient approach. So far, few reports regarding ML-based implementations on parameter-optimization studies have been investigated for SPR-based sensor designs.

Nonetheless, these are mainly centered around Au-based and Ag-based prismatic configurations [6] [7].

In this work, ML-based algorithms are applied to Al-based Kretschmann configurations. An effective ML implementation needs a substantial dataset spanning across a full range of lower and upper bounds. In this view, the plasmonic behavior of Al is appreciable across the entire near-infrared (NIR) range, as has already been highlighted previously by our group [8]. Thus, the focus here is on compiling the optical performance parameters for an Al-Silicon (Si)-Fluorinated Graphene (FG) based SPR sensor within the range of 900 nm to 1500 nm, evaluated across a broad range of geometric dimensions for each of the intermediate parameters. The output sensing parameters are defined in terms of sensitivity (°/RIU) and Figure of Merit [FOM] (1/RIU). Thereafter, the ML implementation is used to predict performance metrics over trained data throughout the NIR range.

Device engineering can only be implemented via ML when consistent physics is involved in the plasmonic interaction at the nano-scale level. Thus, we have considered capturing the predicted results in a specific frequency range only, i.e., the NIR region. Once newer and smaller databases are generated and models are established, ML can enable rapid prediction and optimization of newer/unknown geometrical configurations with minimized computational overhead.

Regression methods like Artificial Neural Networks (ANN), Random Forest, and XG Boost are employed to enhance the sensor's analytical capabilities. ANN captures the non-linear plasmonic behavior with high accuracy. Meanwhile, XGBoost and Random Forest have better interpretability and faster training [9]. Following the data preprocessing, when the input features involve Al at 30nm and a wide range of thicknesses of Si and FG at varying refractive indices from

1.33 to 1.37, the target parameter, i.e., FOM, is predicted. Further, evaluation metrics used to justify the model fit are studied in terms of the R^2 score. Additionally, the feature importance for each model depicts the critical drivers of the outcome of the dataset. Novelty versus the prediction error is also observed, showing which models are more robust towards an unknown dataset. In this way, different ML algorithms applied over newer datasets can help devise new approaches to observe existing analytical trends differently. Once a model is trained, it can be used as a surrogate for larger, exhaustive simulation methods (FDTD, FEM) and numerical analysis. This way, analytical design engineering would become more straightforward and efficient.

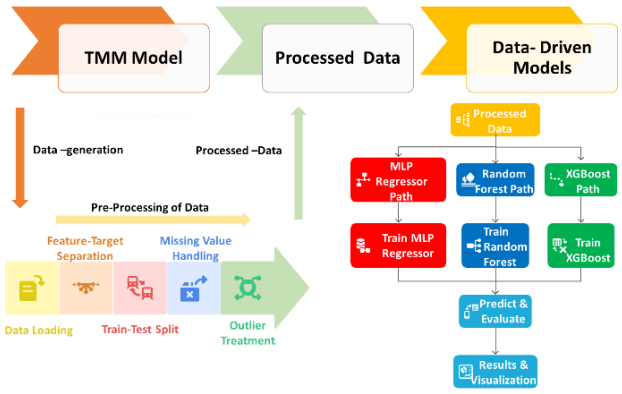

Fig. 1 Steps involved from TMM simulations to Analysis based on ML models

Figure 1 illustrates the workflow carried out in this article. It consists of three major blocks. The first block is the Transfer Matrix Method (TMM) model, which is simulated in MATLAB to obtain performance parameters such as sensitivity, full width at half maximum (FWHM), minimum reflectance (R_{min}), and figure of merit (FOM). These simulations are iterated hundreds of times to generate a comprehensive dataset. The generated data is then preprocessed and subsequently fed into the last block, where different data-driven machine learning models are analyzed for their efficient design approach. The ML approach can help enhance the efficiency of the plasmonic configurations once the models are well-trained. Eventually, future scope involves realizing the inverse design problem, starting with a desirable response per the application and aiming to find an optimized geometrical structure to produce it. This added advantage was not previously the case in analytical design engineering.

2. SENSOR DESIGN AND OPTIMIZATION

The methodology used to achieve the final optimized plasmonic design involves a two-step approach:

2.1 Transfer Matrix method (TMM) for Al-based Prism configuration:

Firstly, Drude's model is used to calculate the dielectric constant (ε_m) of Al using Eq. (1).

$$\varepsilon_m(\lambda) = 1-\left(\frac{\lambda^2\lambda_c}{\lambda_p^2(\lambda_c+j\lambda)}\right) \quad (1)$$

Where λ is the wavelength, $\lambda_p = 1.0657e^{-7}$ m and $\lambda_c = 2.4511e^{-5}$ m denote the plasma wavelength and collision wavelength, respectively. Furthermore, the refractive indices for Si and Gr (in the NIR range) utilized to reach the optimized plasmonic design are extracted from Ref. [10] and [11], respectively.

When several homogeneous layers are aligned along the z-axis, reflectance is calculated using the TMM methodology [12]. The coefficient of total reflection is computed using the N-layer approximation approach. To relate the initial and final electric and magnetic tangential field components, we computed a characteristic matrix M for the kth layer, which has the refractive index n_k.

Three primary metrics- sensitivity, minimum reflectance, and FOM are used in the sensor's design to assess its optical performance. The ratio of the change in resonance angle to the change in the analyte's refractive index is known as sensitivity. The breadth of the resonance curve at 50% of the reflected intensity is known as the Full Width Half Maximum (FWHM), and it gives information about how sharp the resonance is. The ratio of sensitivity to FWHM is used to compute the FOM.

2.2 ML-based approach for Parameter Optimization

We employed three machine learning models: an Artificial Neural Network (ANN) for capturing high-dimensional nonlinear dependencies, and two ensemble-based techniques- Random Forest and XGBoost for their robustness to noise, interpretability, and efficiency in handling smaller datasets.

The data-set with 1000 entries (curated from TMM technique) was pre-processed using feature scaling, and split into training and testing subsets (80:20). The approach involved calculating the FOM prediction problem as a regression task, where key design parameters such as geometry and material properties served as input features, and plasmonic responses (e.g., resonance wavelength or field enhancement) were the target outputs. All three ML models were implemented using Python with libraries including scikit-learn, XGBoost, and TensorFlow/Keras. The predictions were validated against known physical behavior to ensure consistency with the underlying plasmonic theory. The reliability of the models applied was evaluated using the standard regression metric: coefficient of determination (R^2) [13]. This methodology provides a scalable framework for rapid prototyping and inverse design of plasmonic systems, potentially applicable to a wide range of nanophotonic structures.

3. RESULTS AND DISCUSSIONS

The plasmonic resonance is initiated with the optimization of Al in a multi-layer homogenous structure arranged over a prism (CaF_2 (n = 1.426)) interface. Because of its chemical inertness, a CaF_2 prism is selected for effective coupling of p-polarized incident light [14]. In steps of 10nm, the optimized Al thickness stands at 30nm when optimized in the range from 20nm to 50nm. Figure 2(a) shows the considered schematic (not to scale) of the Al-Si-FG-sensing medium in a prism-based design. Figures 2(b- d) depict the universal plasmonic nature of Al in the entire NIR regime ((b) 900nm, (c) 1100nm, and (d) 1500nm). The prism-based design shows multiple resonance dips, which are waveguide modes and the SP modes, when the light is incident at angles beyond the critical angles of reflection under the attenuated total internal reflection phenomenon. The dips represented are at an optimized thickness of 10 nm of Si and 0.34 nm of FG.

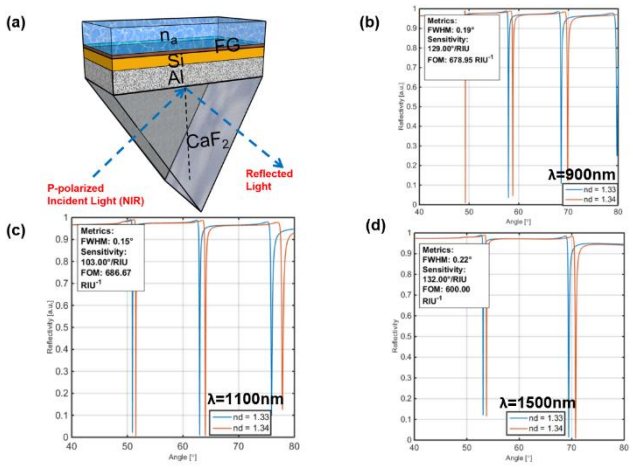

Fig. 2 (a) Schematic of Al-based three-layered Prism configuration; Reflectivity dips showing the plasmonic nature of Al thickness of 30nm covering a broad range of NIR regime at wavelengths of (b) 900nm, (c) 1100nm, and (d) 1500nm, respectively.

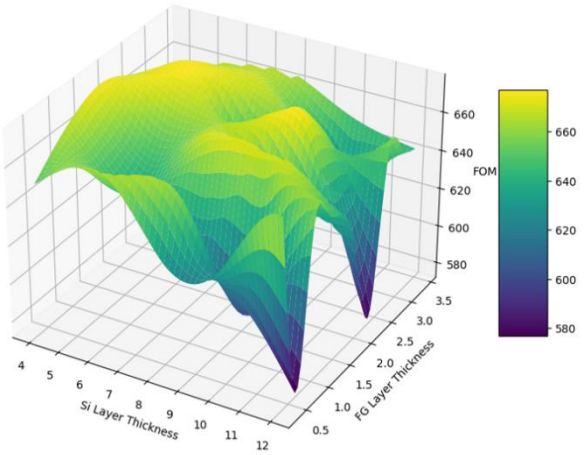

Fig. 3 3D surface plot of FOM as a function of Si and FG layer thickness

Further studying the pattern of the compiled dataset of varied thickness of Al-Si-FG shows that the FOM, i.e., the target feature, exhibits a highly non-linear behavior. In this view, Figure 3 exhibits such behavior, characterized by multiple peaks and valleys, thereby presenting a complex interdependence between Si layer thickness and FG layer thickness in obtaining the FOM. The yellow ridges indicative of high FOM suggest specific combinations of these parameters that lead to optimal output performance. On the other hand, the lower FOM regions (purple troughs) emphasize the configurations of device designs with reduced FOM. This intricate landscape necessitates advanced optimization methods like ML to explore the parameter space efficiently.

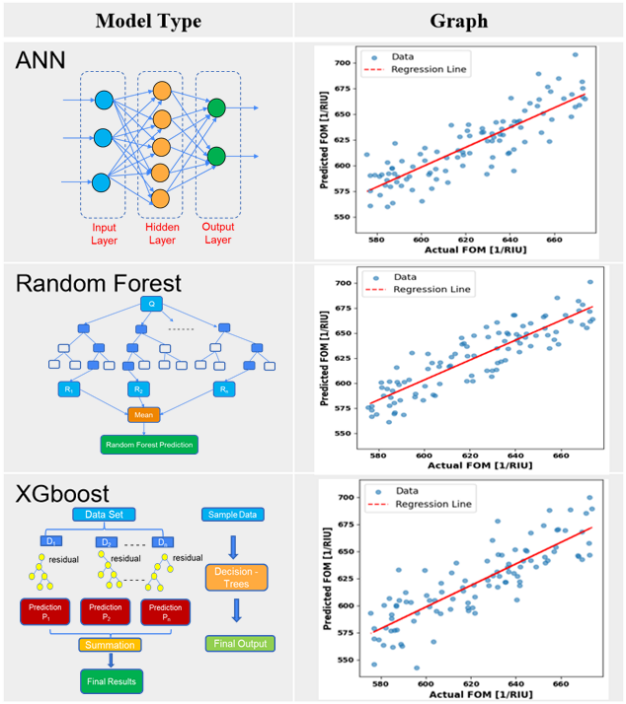

Fig. 4 Predicted v/s Actual FOM Using ANN, Random Forest, and XGBoost Models.

Next, regression techniques are applied that can generalize complex input-output mappings in non-linear plasmonic interactions. We have computed the R^2 score for three different regression models for this.

Herein, the R^2 score is defined as:
$R^2 = 1 - (\text{sum squared regression (SSR)} / \text{total sum of squares (SST)})$
$R^2 = 1 - (\sum (y_i - \hat{y}_i)^2 / \sum (y_i - \bar{y})^2)$

Where y_i is the actual value, $\hat{y}_i$ is the predicted value, and $\bar{y}$ is the mean of actual values. The R^2 score ranges from 0 to 1, where an R^2 score of 1 indicates that all the variations in y are fully explained by the model (perfect fit), while an R^2 score tending towards zero indicates that the model explains none of the variations in y. Figure 4 illustrates how well each model's predictions match the actual values in this context. The red lines signify the regression trend line, while the blue dots represent the data points. Each scatter plot illustrates the relationship between the actual and predicted FOM values. Ideally, the red line must closely align with correct predictions. Random Forest

and ANN show minimal scatter around the regression line. On the other hand, XGBoost shows slightly higher dispersion with a broader spread around the regression line.

A bar chart comparison of the R^2 scores calculated for each of the regression models above is presented in Figure 5. Among them, Random Forest achieved the highest R^2 score of 0.78, indicating the best performance in explaining the variance in the target variable. ANN followed with a score of 0.736, and XGBoost with the lowest score of 0.724. This shows that Random Forest and ANN are more reliable in predicting FOMs for different plasmonic setups. XGBoost underperforms here, possibly due to differences in data splitting, tuning, or sensitivity to outliers. The bar plot comparison emphasizes the need for continued data collection and refinement of the input feature to improve the R^2 score further.

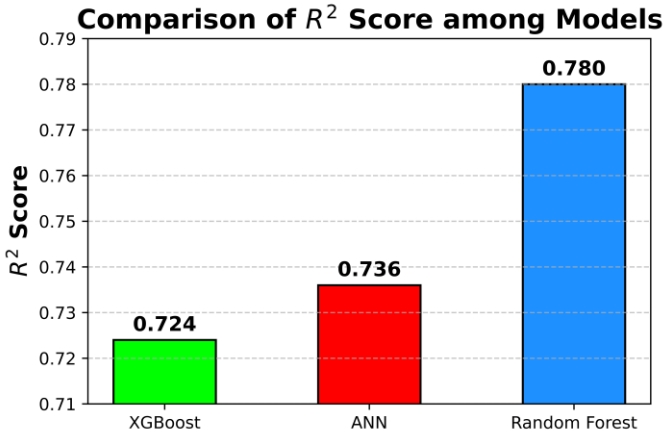

Fig. 5 Bar plot comparison of R^2 score for the three regression models

Next, the feature importance for each of the models is discussed. This is because the geometrical optimization comes secondary as the primary drivers of sensor design are operating wavelength and material selection. In this regard, the feature importances obtained from three distinct models-XGBoost, Random Forest, and Multi-Layer Perceptron (MLP), utilizing permutation importance are compared in Figure 6, providing information about the main factors influencing the model predictions.

The refractive index is the most significant feature in all three models, suggesting a close relationship between this variable and the desired attribute. This consistency across various model architectures implies that the refractive index captures a key component of the underlying physical behavior that the models are learning. The fact that wavelength is the second most crucial characteristic in every situation highlights its essential function, most likely because it affects optical response or material interaction.

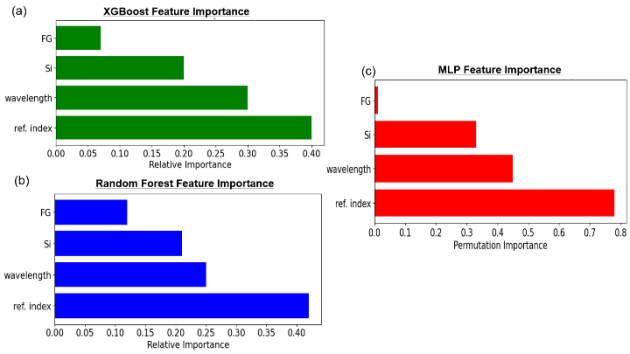

Fig. 6 Comparison of feature importance across models: (a) XGBoost, (b) Random Forest, and (c) MLP{ANN}

Across all models, the Si feature has a moderate level of relevance and makes a significant but not overwhelming contribution to prediction accuracy. On the other hand, FG has the lowest value, particularly in the MLP model, where its permutation importance is almost zero. This implies that FG has little predictive value and could be a good candidate for feature reduction or additional research on its applicability.

In summary, Figure 6 shows that wavelength and refractive index are the key variables influencing model performance, with FG providing the least impact and Si providing moderate Si dependence. In applications where the comprehension of physical factors is just as crucial as accuracy, these insights not only direct future feature engineering endeavors but also improve interpretability and the model's predictions.

In the context of physics-based machine learning challenges, a novelty is the degree to which a model maintains its robustness when it comes to encountering data that is different from the training set. Figure 7 compares prediction error versus novelty for the above-discussed models. Although there is still considerable diversity in prediction errors, the ANN model shows some resilience to new inputs among the models examined. On the other hand, XGBoost shows a more noticeable decline in predicting performance and is more sensitive to unknown data. Likewise, the Random Forest model's accuracy decreases with growing data unfamiliarity, as evidenced by the positive connection between novelty and prediction error. These patterns emphasize the importance of assessing model reliability in novel situations, especially in scientific applications where predictability and interpretability are crucial. These ML-based analyses offer one key advantage: they provide newer dimensions and novel perspectives to plasmonic engineering that were previously unexplored when investigating through traditional data-driven methods.

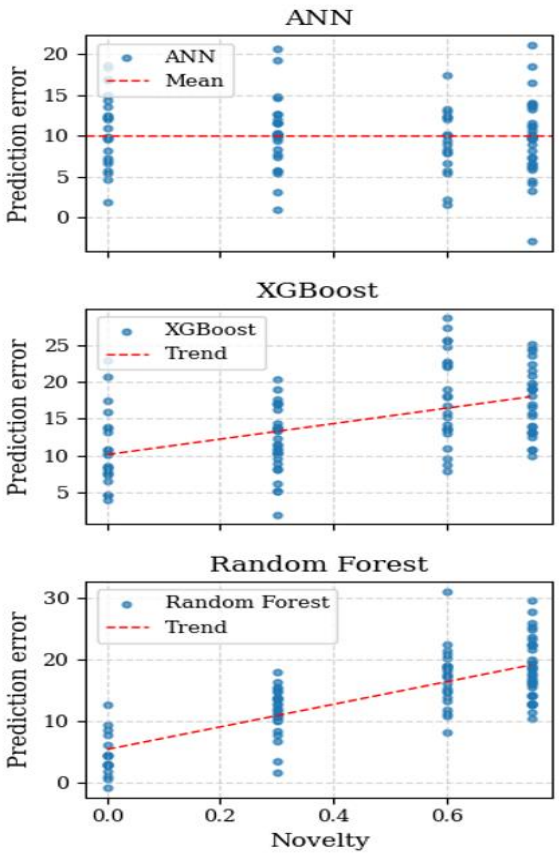

Fig. 7 Relationship between prediction error and data novelty across all the ML models

Table I Comparison of Previously Reported Works

Ref.	λ [nm]	Metal	Sensitivity (°/RIU)	Sensitivity (nm/RIU)	FOM (RIU^{-1})
[15]	Visible region	Prism-SPR with Gr and PSO optimization	68.75	-	100
[16]	720-1280	PCF-SPR with Au nanowires	-	2000–18000	311.41
[17]	800-1600	D-Shaped Fiber with Grated Au-ZnS	-	9000 – 18,000	158.73
[18]	1870-1950	square-shaped within an incomplete circle refractive index biosensor (SWICRIB)	700	-	298.81
[19]	1000-2800	MMF-SPR Biosensor	-	31,427	271.43
[20]	20-180	PCF-SPR biosensor	-	18,000	125
This work	900-1550	Al-Si-FG	132	-	600

The tabulated entries in Table I show limited reports of Au and Ag-based designs using the ML-based approach to predict either the resonance wavelength or performance parameters. In contrast, most earlier works are limited to traditional optimization-based methods, whereas recent works are utilizing the ML-based approach. In this view, an Al-based SPR sensor in which resonance wavelength and performance parameters are optimized and predicted using different ML techniques, with the help of our own dataset, though in the future we will expand the dataset so that data-driven techniques can be used with more accuracy and precision.

4. CONCLUSIONS

The curated dataset enables the use of an inverse design approach in future research, representing a significant advancement over conventional optical performance monitoring techniques.

Due to its relative novelty, the Al-based dataset is a valuable starting point for upcoming models and analysis, especially in application-specific fields where sparse data is typical. In this regard, the model's remarkable performance and ability to generalize successfully despite data constraints are highlighted by its R^2 score. In addition to measurements, this result highlights significant insights into underlying trends, correlations, and hypotheses, proving the model's capacity to capture intricate interactions in a data-scarce condition.

REFERENCES

[1] N. Khansili, G. Rattu, and P. M. Krishna, "Label-free optical biosensors for food and biological sensor applications," *Sensors Actuators, B Chem.*, vol. 265, pp. 35–49, 2018, doi: 10.1016/j.snb.2018.03.004.

[2] J. Homola, "Optical fiber sensor based on surface plasmon excitation," *Sensors Actuators B. Chem.*, vol. 29, no. 1–3, pp. 401–405, 1995, doi: 10.1016/0925-4005(95)01714-3.

[3] F. Yan *et al.*, "Ultrasensitive Tunable Terahertz Sensor with Graphene Plasmonic Grating," *J. Light. Technol.*, vol. 37, no. 4, pp. 1103–1112, 2019, doi: 10.1109/JLT.2018.2886412.

[4] M. B. Hossain, "Graphene-MoS2-Au-TiO2-SiO2 Hybrid SPR Biosensor For Formalin Detection: Numerical Analysis And Development," *Adv. Mater. Lett.*, vol. 10, no. 9, pp. 656–662, 2019, doi: 10.5185/amlett.2019.0001.

[5] S. B. Saadatmand, V. Ahmadi, and S. M. Hamidi, "Resonant field enhancement in all-dielectric metastructures supporting THz bound states in the continuum," in *Conference on Millimeter-Wave and Terahertz Technologies, MMWaTT*, 2022, pp. 1–5, doi: 10.1109/MMWaTT58022.2022.10172121.

[6] S. K. Patel, S. Member, J. Surve, A. Baz, and S. Member, "Optimization of Novel 2D material based SPR Biosensor using Machine Learning," *IEEE Trans. Nanobioscience*, vol. PP, p. 1, 2024, doi: 10.1109/TNB.2024.3354810.

[7] G. Ansari, A. Pal, A. K. Srivastava, and G. Verma, "Sensing and Bio-Sensing Research Machine learning approach to surface plasmon resonance bio-chemical sensor based on nanocarbon allotropes for formalin detection in water," *Sens. Bio-Sensing Res.*, vol. 42, no. November, p. 100605, 2023, doi: 10.1016/j.sbsr.2023.100605.

[8] S. Shukla and P. Arora, "Aluminum as a competitive plasmonic material for the entire electromagnetic spectrum: A review," *Results Opt.*, vol. 18, no. November 2024, p. 100760, 2025, doi: 10.1016/j.rio.2024.100760.

[9] Y. Ş. Türker, Ş. Kilinçarslan, and E. Y. Ince, "Performance of ANN, Random Forest and XGBoost methods in predicting the flexural properties of wood beams reinforced with carbon-FRP," Wood Material Science & Engineering, vol. 20, no. 3, pp. 657–668, 2024. doi: 10.1080/17480272.2024.2370942.

[10] M. A. Green, "Self-consistent optical parameters of intrinsic silicon at 300 K including temperature coefficients," *Sol. Energy Mater. Sol. Cells*, vol. 92, no. 11, pp. 1305–1310, 2008, doi: 10.1016/j.solmat.2008.06.009.

[11] S. Shukla and P. Arora, "Investigation of 2D nanomaterials on MXene (Ti3C2Tx)-based aluminum plasmonic devices for biosensing in the near-infrared region," *Appl. Phys. A Mater. Sci. Process.*, vol. 128, no. 9, pp. 1–9, 2022, doi: 10.1007/s00339-022-05947-6.

[12] S. Shukla, N. Grover, and P. Arora, "Resolution enhancement using a

multi-layered aluminium-based plasmonic device for chikungunya virus detection," *Opt. Quantum Electron.*, vol. 55, no. 3, pp. 1–10, 2023, doi: 10.1007/s11082-022-04485-y.

[13] L. S. P. Maia *et al.*, "Inverse Design of Plasmonic Nanostructures Using Machine Learning for Optimized Prediction of Physical Parameters," *Photonics*, vol. 12, no. 6, p. 572, 2025, doi: 10.3390/photonics12060572.

[14] A. K. Pandey and A. K. Sharma, "Simulation and analysis of plasmonic sensor in NIR with fluoride glass and graphene layer," *Photonics Nanostructures - Fundam. Appl.*, vol. 28, pp. 94–99, 2018, doi: 10.1016/j.photonics.2017.12.003.

[15] K. Rastogi, A. K. Sharma, and Y. K. Prajapati, "Demonstration of graphene-assisted tunable surface plasmonic resonance sensor using machine learning model," *Appl. Phys. A*, vol. 129, no. 5, p. 351, 2023, doi: 10.1007/s00339-023-06630-0.

[16] A. Ehyaee, A. Rahmati, A. Bosaghzadeh, and S. Olyaee, "Machine learning-enhanced surface plasmon resonance based photonic crystal fiber sensor.," *Opt. Express*, vol. 32, no. 8, pp. 13369–13383, Apr. 2024, doi: 10.1364/OE.521152.

[17] Banerjee, Ananya & Jaisingh Thangaraj. "SPR-based refractive index sensor design with grated Au-ZnS for dengue detection using machine learning." Spectrochimica Acta Part A: Molecular and Biomolecular Spectroscopy, 2025: 10.1016/j.saa.2025.126276

[18] Y. A. A. Ali et al., "Design and analysis of surface plasmon resonance-based refractive index biosensor for detection of colorectal cancer with machine learning approach," Plasmonics, 2025, pp. 1–13, doi: 10.1007/s11468-024-02720-8

[19] R. Rahul, A. Banerjee, and J. Thangaraj, "Bayesian regularized neural network based SPR biosensor for early cancer detection," IEEE Sensors J., 2025, doi: 10.1109/JSEN.2025.3577936.

[20] L. Guedri-Knani, S. Kaziz, and C. Dridi, "Performance prediction of a highly sensitive optimized PCF-SPR biosensor for cancer cell detection using MLP-based ANN model," IEEE Sensors J., 2025, doi: 10.1109/JSEN.2025.3556292.

AUTHORS:

R. Runthala (Student Member, IEEE) received his B.E. degree in electronics and communication engineering from JECRC, Jaipur, in 2009. He worked at CEERI-Pilani as a Project Assistant in Testing and Designing of B-Type Cathodes for TWT applications. He worked as a Lecturer and Assistant Professor at the BK Birla Institute of Engineering and Technology (BKBIET), Pilani, from 2011 to 2023. He is working toward a PhD in the Department of Electrical & Electronics Engineering, Birla Institute of Technology and Science, Pilani, India. His research work mainly focuses on Optimizing the design of SPR-based optical sensors.

E-mail: p20230044@pilani.bits-pilani.ac.in

Dr. Pankaj Arora (Senior Member, IEEE) received his M.S. and PhD dual degree in Electrical Engineering from IIT Madras, Chennai, India, in 2016. From 2016 to 2018, he was a Post-Doctoral Researcher at the Faculty of Science, The Hebrew University, Jerusalem, Israel, where he was involved in studying the light-matter interaction at the nanoscale in photonic devices. He is an assistant professor at the Department of Electrical and Electronics Engineering, Birla Institute of Technology and Science at Pilani, India. His current research interests include plasmonics, silicon photonics, optical sensors, 2D nanomaterials, microfluidics, VLSI Design, and imaging microscopy.

Corresponding author E-mail: pankaj.arora@pilani.bits-pilani.ac.in